GSA Data Repository 2020010

A 1.25 Ga depositional age for the "Paleoproterozoic" Mapedi red beds, Kalahari Manganese Field, South Africa: New constraints on the timing of oxidative weathering and hematite mineralization

by Birger Rasmussen, Janet R. Muhling, Jian-Wei Zi, Harilaos Tsikos and Woodward Fischer

SAMPLE DESCRIPTIONS

To date the Mapedi Formation in the Kalahari Manganese Field, Griqualand West, South Africa, 28 samples were collected from drill-core from drill-hole W270 north of Hotazel. The drill-hole intersected the top of the Ongeluk Formation, Hotazel Formation and Mapedi-east Formation. A felsic tuff and samples of sandstone were chosen for U-Pb geochronology based on the abundance of zircons. Petrographic descriptions of the geochronological samples are given below:

Drill-hole W270, 184.1 m (Quartz arenite)

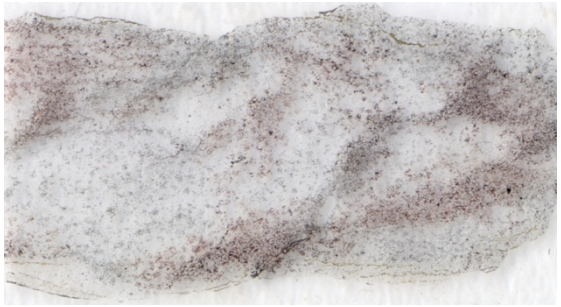

The drill-core sample from drill-depth 184.1 m is a fine-grained quartz arenite. Quartz grains are mostly 0.1-0.2 mm in diameter, but may be up to 0.5 mm in size. Most grains are sub-rounded to well rounded, and commonly have syntaxial quartz overgrowths. Grain contacts vary from planar to concavo-convex, and are micro-stylolitic near clay laminae. Authigenic pyrite is common as small irregular crystals (<10 μm) around quartz grain boundaries. Pyrite also occurs as larger euhedral crystals (up to 50 μm) and fills hairline fractures cross-cutting quartz grains. In places, pyrite occurs as intergranular cement between quartz grains, and has been partly oxidized and replaced by goethite, indicating that the sulfide was originally more abundant. Fine-grained sericite is common as an interstitial matrix between quartz grains. The sandstone also contains trace amounts of detrital muscovite, zircon, tourmaline, rutile, chromite, Ti-oxides and Fe-Ti oxides.

Drill-hole W270, 202.1 and 205.9 m (Very fine-grained sandstones)

The drill-core sample from drill-depth 202.1 m comprises a thinly bedded, fine-grained sandstone and coarse-grained siltstone. Quartz grains range from sub-angular to well rounded, and vary between 0.01-0.3 mm in size. The quartz grains occur in a fine-grained matrix of sericite along with trace amounts of detrital muscovite, biotite, zircon, tourmaline, rutile, apatite and Fe-Ti oxide grains. Diagenetic siderite crystals are common. Pyrite occurs as thin anastomosing streaks. Thin, bedding-parallel particles of kerogen (up to 20 μm in length) occur in some layers of siltstone.

Drill-hole W270, 229.9 m (Felsic tuff)

The drill-core sample from drill-depth 229.9 m contains a ~3 cm thick felsic tuff bed between cream-colored mudstones. The tuff bed contains euhedral zircon crystals (up to 50 µm in size) as well as angular quartz grains. Most of the zircon grains occur in the bottom 1 cm of the bed. Quartz grains vary from 0.1-0.2 mm in diameter at the base of the bed, to <0.05 mm at the top of the tuff. Other constituents include trace amounts of Ti-oxides, Ti-Fe-oxides, apatite, biotite and chlorite. Biotite grains appear to have been replaced by chlorite. The coarser grained crystals appear to float in a matrix of fine-grained sericite. The tuff bed contains abundant siderite rhombs (mostly 0.1-0.2 mm in size), which enclose framework grains. The tuff bed is cross-cut by several fractures (up to 50 µm wide), which contain quartz, chlorite, pyrite, apatite and carbonate.

Drill-hole W270, 283.3 m (Very fine-grained red and green sandstone)

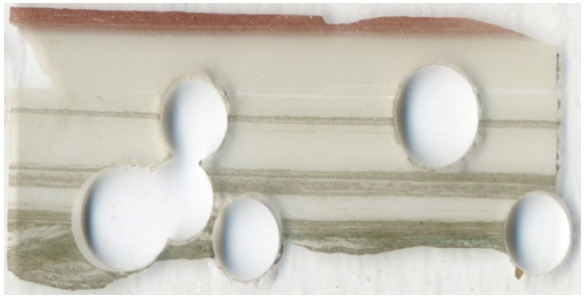

The drill-core sample from drill-depth 283.3 m comprises laminated mudstone with layers of very fine-grained sandstone and coarse-grained siltstone. Quartz grains are angular and are typically 0.1-0.01 mm in size. The quartz grains occur in a matrix of fine-grained muscovite along with trace amounts of detrital zircon, tourmaline, apatite, rutile, and altered Fe-Ti oxide grains. Detrital zircon crystals are concentrated in layers of fine-grained sandstone. Layers of red-colored mudstone contain abundant minute (<1 µm) particles of hematite finely dispersed throughout the sericite matrix. The hematite-bearing layers are locally discordant to sedimentary bedding. The sample also contains several bedding-parallel veins, comprising coarse-grained aggregates of chlorite. Thin (<1 µm) veinlets of pyrite occur along bedding.

Drill-hole W270, 296.1 m (Coarse-grained sandstone)

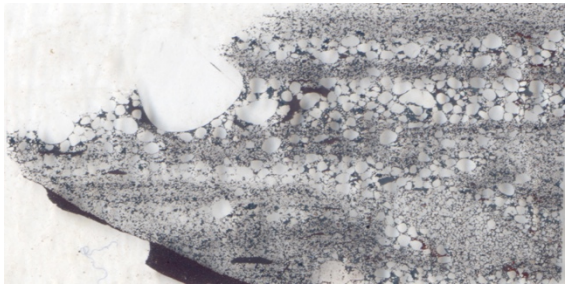

The drill-core sample from drill-depth 296.1 m comprises interbedded fine-grained and coarse-grained sandstone. Detrital quartz grains are typically between 0.1 to 2.0 mm in diameter (some grains are up to 7 mm in diameter). The quartz grains are rounded to well rounded, and many have syntaxial quartz outgrowths. Interstitial spaces between quartz grains are either filled by a matrix of fine-graineD muscovite (sericite) or hematite cement. Rounded zircon grains (up to 0.25 mm in diameter) occur as detrital minerals along bedding surfaces. The sandstones also contain trace amounts of detrital muscovite and tourmaline. The hematite cementation is discordant to bedding, and appears to have formed by replacement of the phyllosilicate matrix.

ANALYTICAL METHODS AND DATA ASSESSMENT

Polished thin sections from the tuff sample were prepared and examined for the presence of zircon using optical and scanning electron microscopes. Zircon crystals were identified and removed for SHRIMP analysis by drilling ~3 mm-diameter plugs from the polished thin sections, and casting the plugs into 25 mm-diameter resin mounts (see Rasmussen and Fletcher, 2010).

Zircon U-Pb analyses were conducted using the sensitive high-resolution ion microprobe (SHRIMP II) instruments in the John de Laeter Centre at Curtin University in Perth, Australia. SHRIMP analyses followed established procedures for small-spot, in situ analysis of zircon extracted from polished thin sections (Rasmussen and Fletcher, 2010). Data were obtained from five analytical sessions using SHRIMP operating parameters listed in Table DR1. Number of scans per analysis was increased to 7-8 to compensate the reduction in primary beam intensity. The Pb/U and U concentration reference standard BR266 (Stern, 2001) and a $^{207}Pb/^{206}Pb$ monitor, OG1 (Stern et al., 2009) were contained on separate mounts that were cleaned and Au-coated together with the sample mounts, and analyzed concurrently with unknown zircons. Throughout most of the analytical sessions, the interpolated analyses from OG1 produced pooled $^{207}Pb/^{206}Pb$ ages within uncertainty of the published reference value (3465.4 ± 0.6 Ma; Stern et al., 2009). However, corrections for IMF were applied to analyses obtained during sessions (i.e., sessions 1 and 5) that yielded OG1 ages show relatively large deviation from the reference value (Table DR1).

Common-Pb corrections were applied to all analyses using contemporaneous isotopic compositions determined according to the model of Stacey and Kramers (1975). Data were reduced using Squid-2 software (Ludwig, 2009) and plots prepared with Isoplot-3 (Ludwig, 2003). Individual analyses are quoted at 1σ uncertainty, whereas weighted mean ages are reported at 95% confidence level.

SHRIMP U-Pb ZIRCON GEOCHRONOLOGY

Felsic Tuff (Drill-hole W270, 229.9 m)

*Z*ircons from the tuff bed are equant to elongate, euhedral to subhedral crystals that are typically 30-50 μm in length (Figs. DR1 and 2). Combining analyses from the 4 sessions, 52 analyses were obtained (Table DR2). These zircon grains contain variably low to moderate U and Th contents (25-597 ppm and 11-631 ppm, respectively), with Th/U ratios varying between 0.24 and 1.44. Sixteen analyses record high proportion of common ^{206}Pb (f_{206} >1%), another 9 analyses are >10% discordant (see footnote in Table DR2 for definition of discordance) although contain <1% common ^{206}Pb. Therefore, these analyses are considered not reliable and are disregarded in age determination. The remaining 27 analyses are concordant or near-concordant (disc. within ± 10%) and contain low common ^{206}Pb (f_{206} ≤1%). They yield ^{207}Pb/^{206}Pb dates ranging from 1836 Ma to 1148 Ma, with a main cluster at the young side. Excluding the 5 analyses that give ^{207}Pb*/^{206}Pb* dates older than 1400 Ma, 22 analyses were obtain from 11 zircon grains and yield a weighted mean ^{207}Pb*/^{206}Pb* date of 1256 ± 26 Ma (MSWD = 1.03). However, it appears that measurement of the ^{238}U/^{206}Pb* ratios for these zircons are with better precision compared with the ^{207}Pb*/^{206}Pb* system (Table DR2). Calculation based on the ^{238}U/^{206}Pb*ratios yielded a weighted mean date of 1245 ± 16 Ma (MSWD = 1.6, n = 21, the youngest analysis is disregarded as a statistical outlier) (Figure DR3). The error is expanded to 20 Ma when including 2σ error of 0.94% in mean U/Pb propagated from the calibration standard BR266. The mean ^{238}U/^{206}Pb* date agrees with the pooled ^{207}Pb*/^{206}Pb* date within uncertainty. Therefore, the more precise ^{238}U/^{206}Pb* date of 1245 ± 20 Ma is taken as the best estimate of the depositional age of the tuff bed.

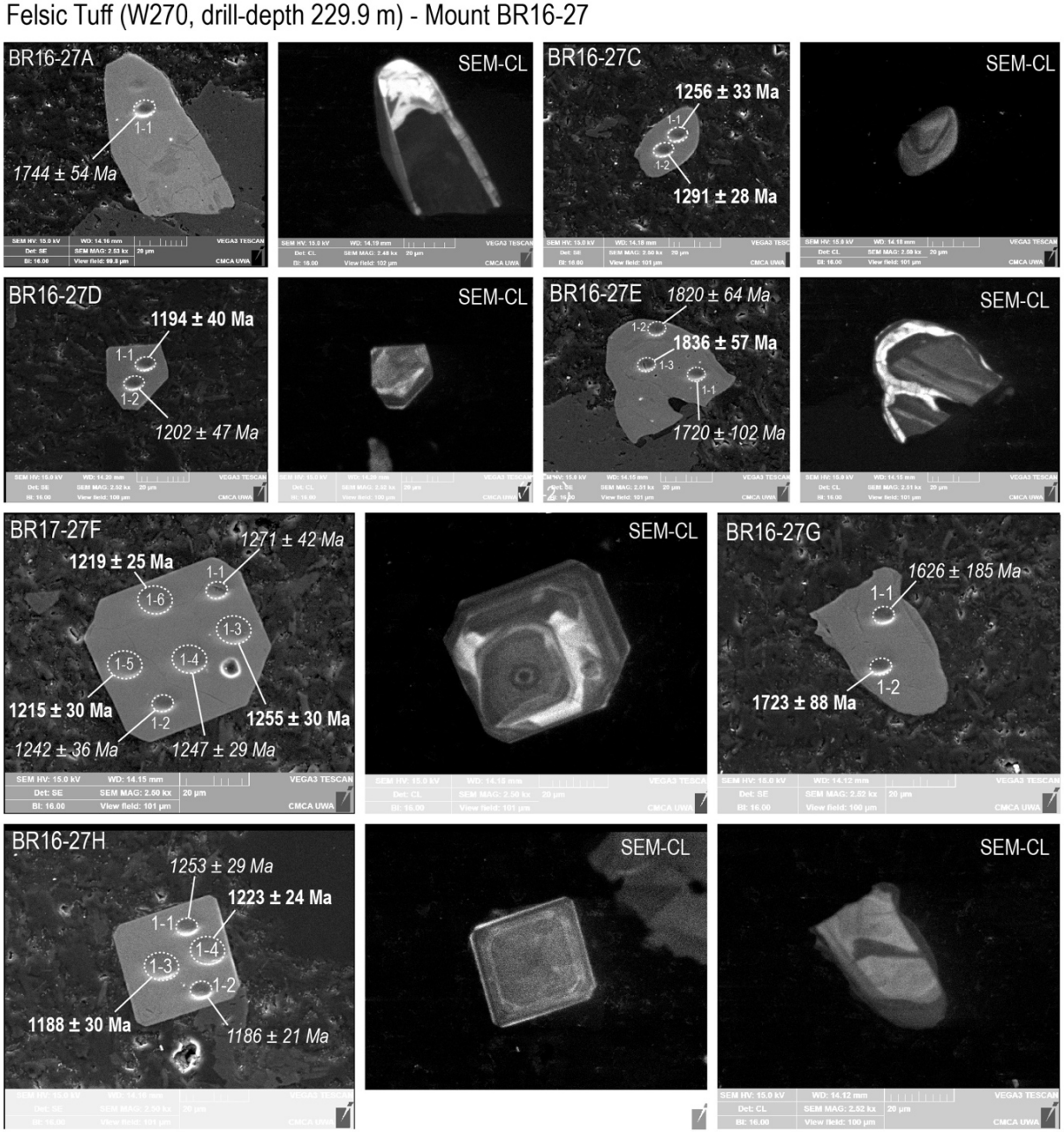

Figure DR1. SEM-backscattered electron (BSE) and cathodoluminescence (CL) images of zircon grains drilled from tuff bed at drill-depth 229.9 m in drill-hole W270 (SHRIMP mount BR16-27 – Table DR2). The oval outlines on zircon grains mark ion microprobe analytical pits and are linked to corresponding $^{207}Pb/^{206}Pb$ or $^{238}U/^{206}Pb^*$ dates with 1σ analytical errors. Numbers in bold represent analyses that were used in age determinations, whereas numbers in italics were not used because of high common Pb contents and/or high levels of discordance.

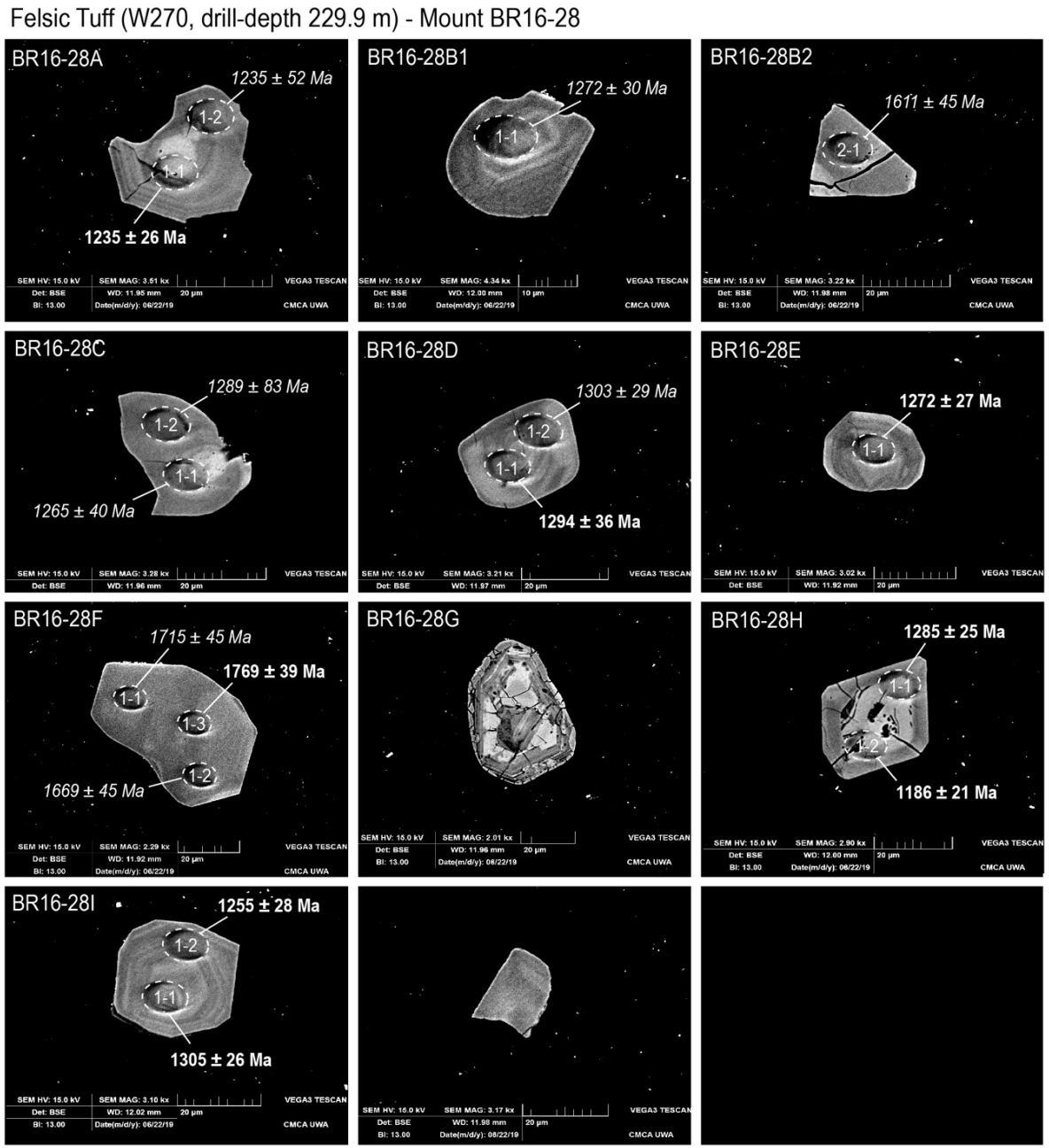

Figure DR2. SEM-backscattered electron (BSE) and cathodoluminescence (CL) images of zircon grains drilled from tuff bed at drill-depth 229.9 m in drill-hole W270 (SHRIMP mount BR16-28 – Table DR2). The oval outlines on zircon grains mark ion microprobe analytical pits and are linked to corresponding $^{207}Pb/^{206}Pb$ or $^{238}U/^{206}Pb^*$ dates with 1σ analytical errors. Numbers in bold represent analyses that were used in age determinations, whereas numbers in italics were not used because of high common Pb contents and/or high levels of discordance.

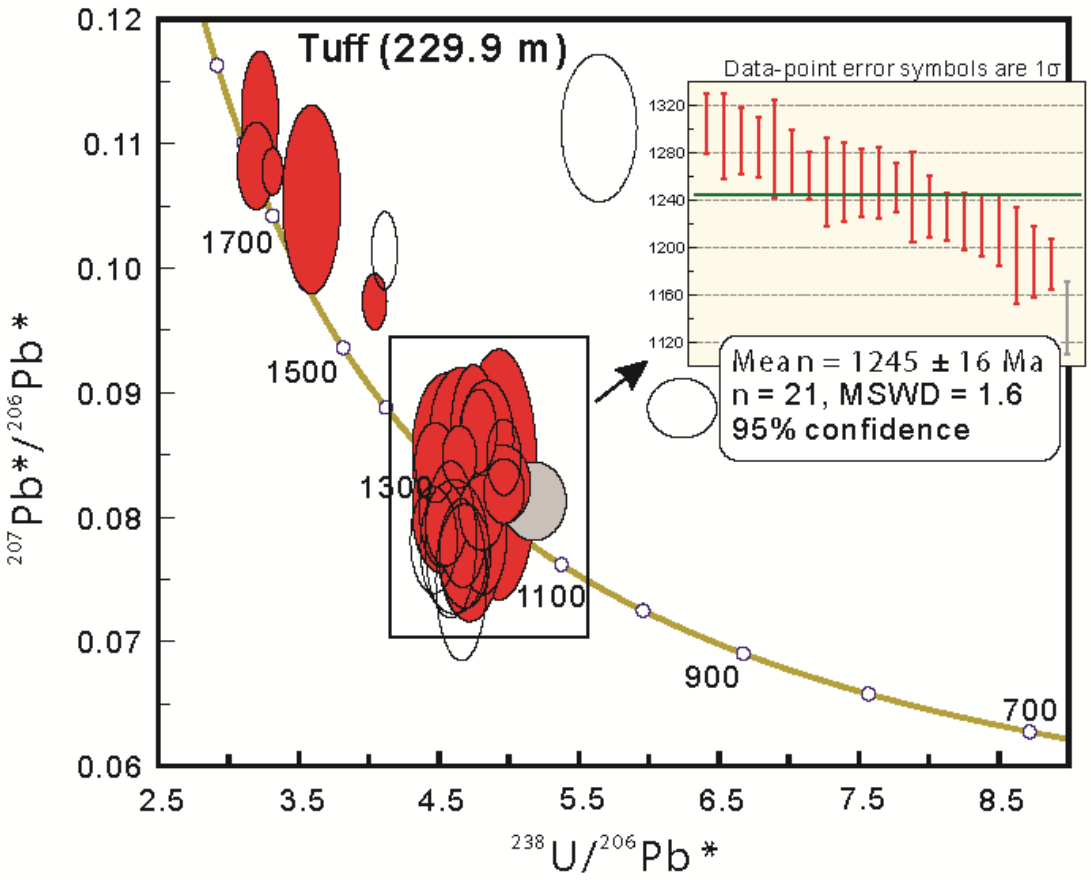

Figure DR3. Concordia plot for U-Pb analyses of zircon in the tuff bed. Unfilled ellipses represent discordant analyses, the grey-shaded ellipse represents a statistical outlier, which were excluded in age calculation. Analyses giving high common Pb are not shown but listed in Table DR2.

Quartz arenite (Drill-hole W270, 184.1 m)

Zircons from the sandstone are typically stubby grains (or crystal fragments) of up to 100 μm long. Most grains appear to have been rounded to variable extent (Figs. DR4 and DR5). Fifty-eight analyses were obtained on zircons from the sandstone sample. Seven of them have common Pb level above the threshold (i.e., f_{206} >1%), whereas another 12 analyses contain <1% common ^{206}Pb but yielded discordant dates (disc. >10%). These analyses are not considered further. The remaining 39 analyses are from 20 zircon grains which yielded ^{207}Pb*/^{206}Pb* dates spanning a wide range from 3139 Ma to 1292 Ma (Table DR5), with a prominent peak at 2077 ± 21 Ma (n = 23, MSWD = 1.2) and several possible subordinate peaks (Fig. DR6). Importantly, the youngest 3 analyses yielded identical ^{238}U/^{206}Pb* and ^{207}Pb*/^{206}Pb* dates at 1300 Ma, within uncertainty of the tuff age.

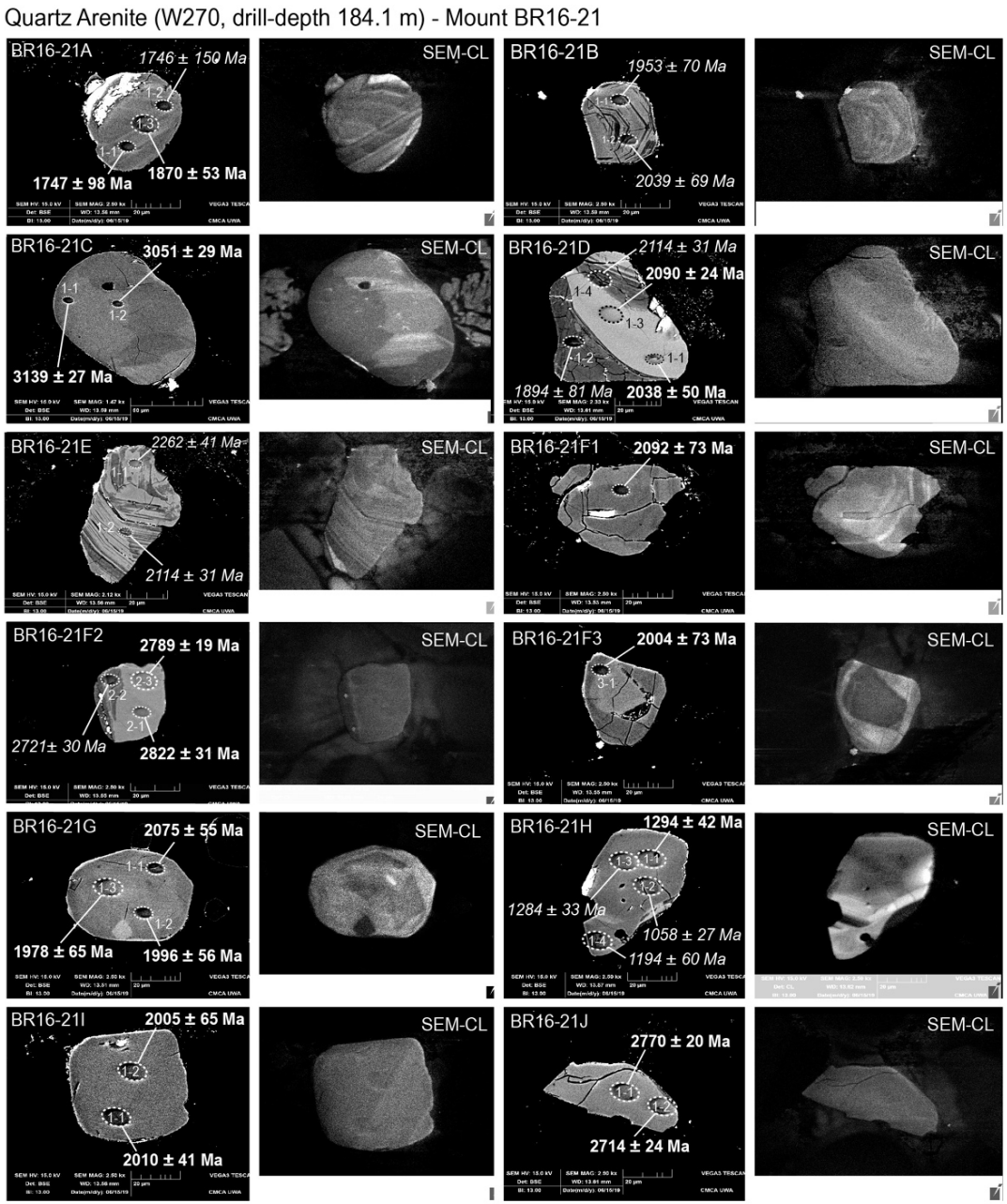

Figure DR4. SEM-backscattered electron (BSE) and cathodoluminescence (CL) images of detrital zircon grains drilled from a quartz arenite at drill-depth 184.1 m in drill-hole W270 (SHRIMP mount BR16-21 – Table DR5). The oval outlines on zircon grains mark ion microprobe analytical pits and are linked to corresponding $^{207}Pb/^{206}Pb$ or $^{238}U/^{206}Pb$* dates with 1σ analytical errors. Numbers in bold represent analyses that were used in age determinations, whereas numbers in italics were not used because of high common Pb contents and/or high levels of discordance.

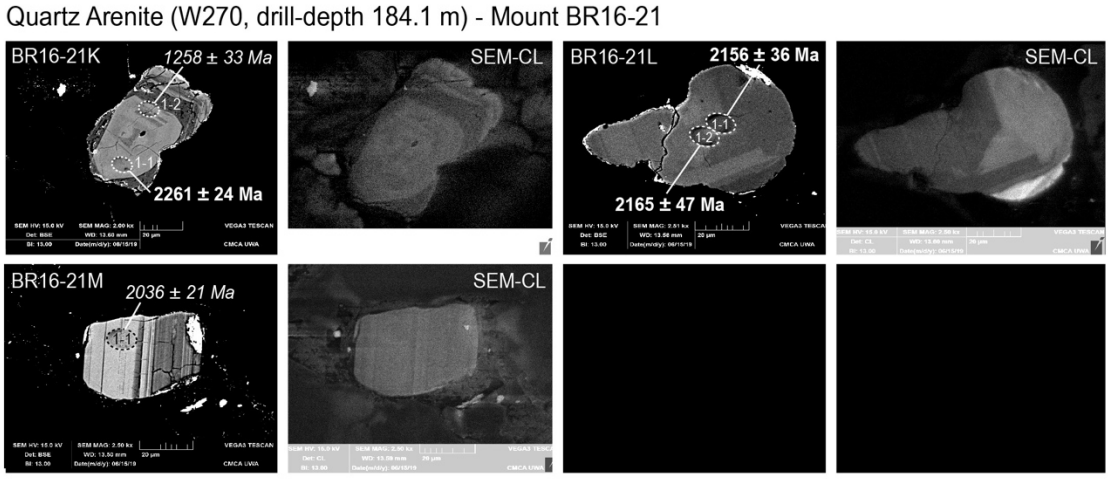

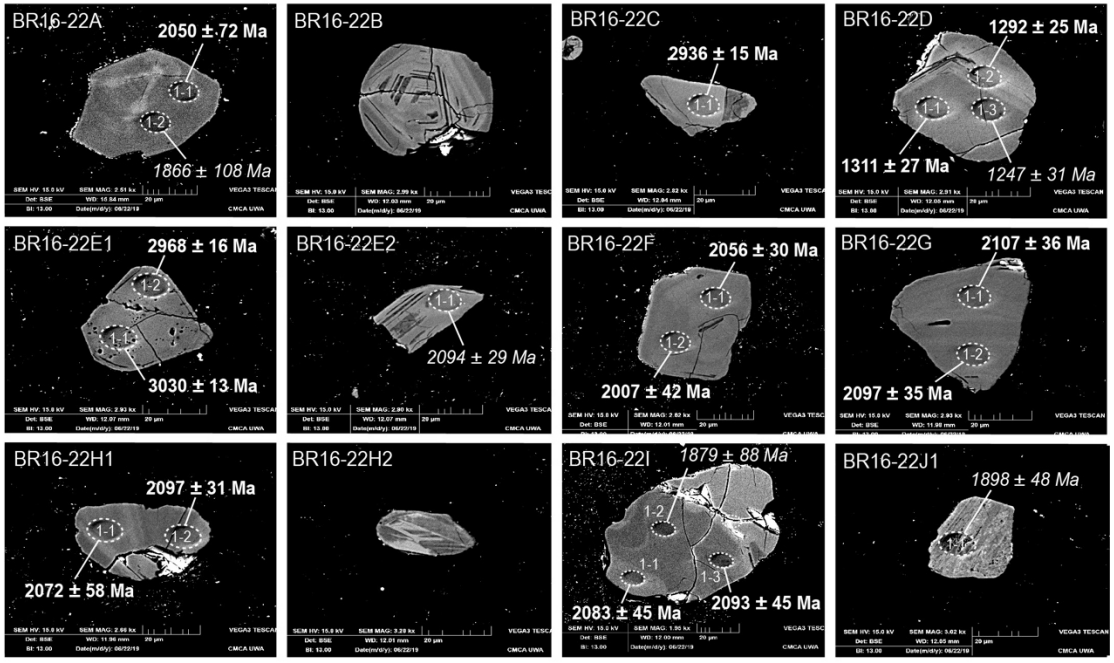

Figure DR5. SEM-backscattered electron (BSE) and cathodoluminescence (CL) images of detrital zircon grains drilled from a quartz arenite at drill-depth 184.1 m in drill-hole W270 (SHRIMP mounts BR16-21 and BR16-22 – Table DR5). The oval outlines on zircon grains mark ion microprobe analytical pits and are linked to corresponding $^{207}Pb/^{206}Pb$ or $^{238}U/^{206}Pb^*$ dates with 1σ analytical errors. Numbers in bold represent analyses that were used in age determinations, whereas numbers in italics were not used because of high common Pb contents and/or high levels of discordance.

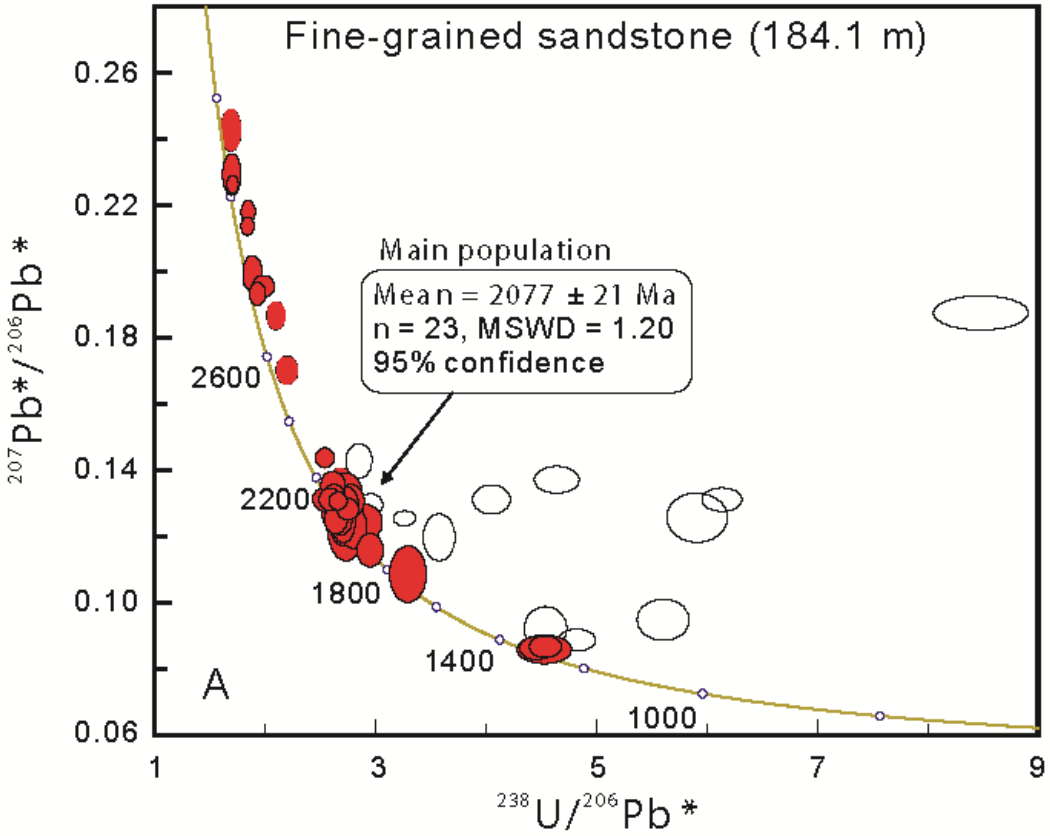

Figure DR6. Concordia plot for U-Pb analyses of zircon from the fine-grained quartz arenite. Unfilled ellipses represent discordant analyses. Analyses giving high common Pb are not shown but listed in Table DR5.

Fine-grained sandstone (Drill-hole W270, 202.1 m and 205.9 m)

Zircon grains from the two samples of fine-grained sandstone are commonly stubby, euhedral to subhedral crystals or fragments of euhedral crystals with visible oscillatory zoning, and are up to 50 μm long (Figs. DR7 and DR8). Combining data from two samples (W270 at drill-depths of 202.1 m and 205.9 m), 30 zircon analyses were obtained during two analytical sessions (Table DR4). Ten analyses contain high common ^{206}Pb (f_{206} >1%), another 4 analyses have f_{206} <1% but are >10% discordant. These analyses are considered unreliable and excluded in age determination. The remaining 16 analyses are concordant or near-concordant (disc. within ± 10%) and have f_{206} <1%. These analyses yield ^{207}Pb*/^{206}Pb* dates ranging from 2799 Ma to 1141 Ma, with 3 distinct age clusters at 2765 Ma (n = 4), 2070 Ma (n = 6), and 1250 Ma (n = 6) (Figure DR3). The ~1250 Ma analyses are from 5 zircon grains which contain higher U and Th concentrations (average 308 ppm vs. 174 ppm, and 280 ppm vs. 116 ppm, respectively) relative to the older zircons. Dates derived from ^{238}U/^{206}Pb* and ^{207}Pb*/^{206}Pb* for this group agree within uncertainty, and are similar to the predominant age of the tuff zircon (Fig. DR9).

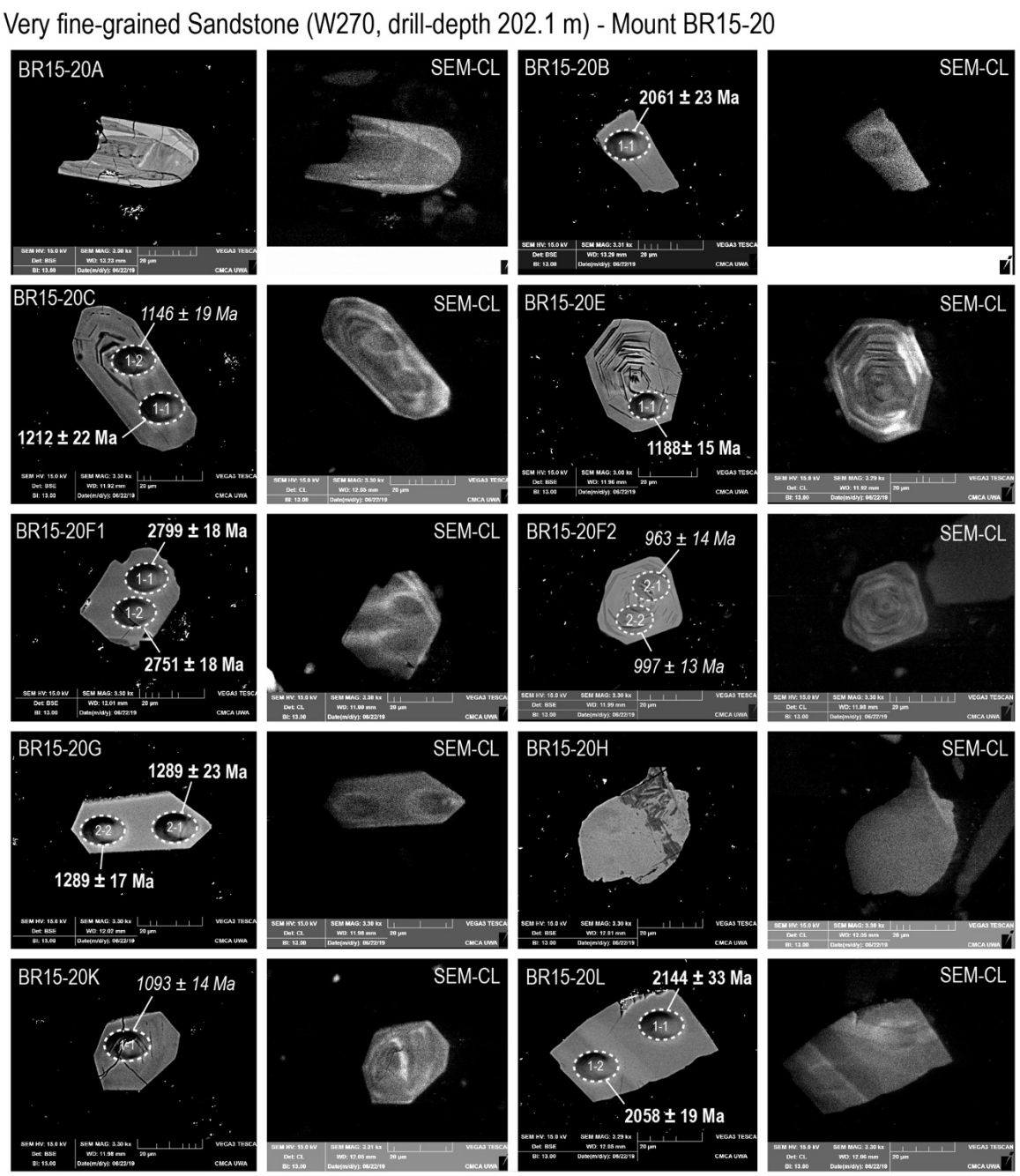

Figure DR7. SEM-backscattered electron (BSE) and cathodoluminescence (CL) images of detrital zircon grains drilled from fine-grained sandstones at drill-depth 202.1 m in drill-hole W270 (SHRIMP mount BR15-20 – Table DR3). The oval outlines on zircon grains mark ion microprobe analytical pits and are linked to corresponding $^{207}Pb/^{206}Pb$ or $^{238}U/^{206}Pb^*$ dates with 1σ analytical errors. Numbers in bold represent analyses that were used in age determinations, whereas numbers in italics were not used because of high common Pb contents and/or high levels of discordance.

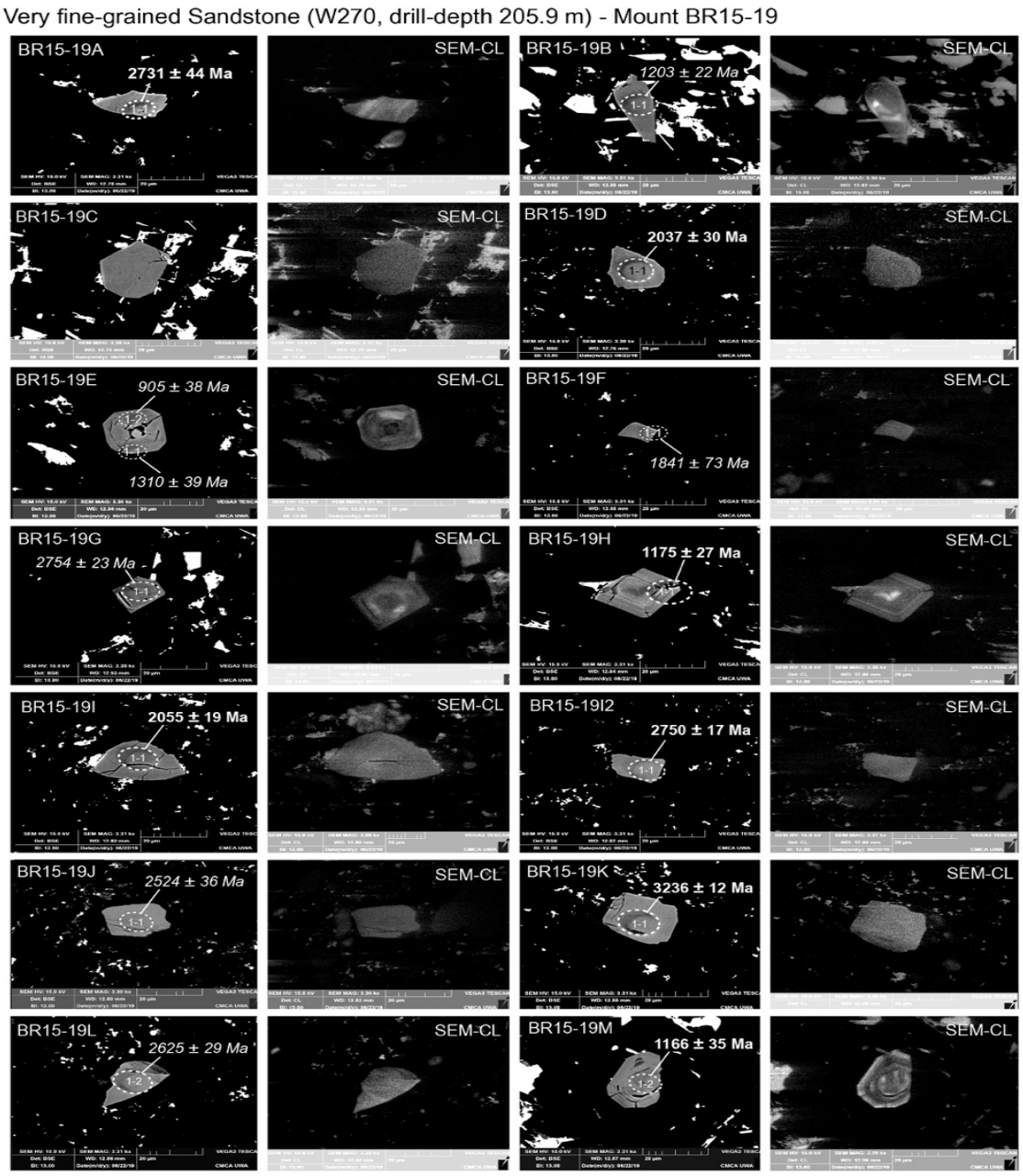

Figure DR8. SEM-backscattered electron (BSE) and cathodoluminescence (CL) images of detrital zircon grains drilled from very fine-grained sandstones at drill-depth 205.9 m in drill-hole W270 (SHRIMP mount BR15-19 – Table DR3). The oval outlines on zircon grains mark ion microprobe analytical pits and are linked to corresponding $^{207}Pb/^{206}Pb$ or $^{238}U/^{206}Pb^*$ dates with 1σ analytical errors. Numbers in bold represent analyses that were used in age determinations, whereas numbers in italics were not used because of high common Pb contents and/or high levels of discordance.

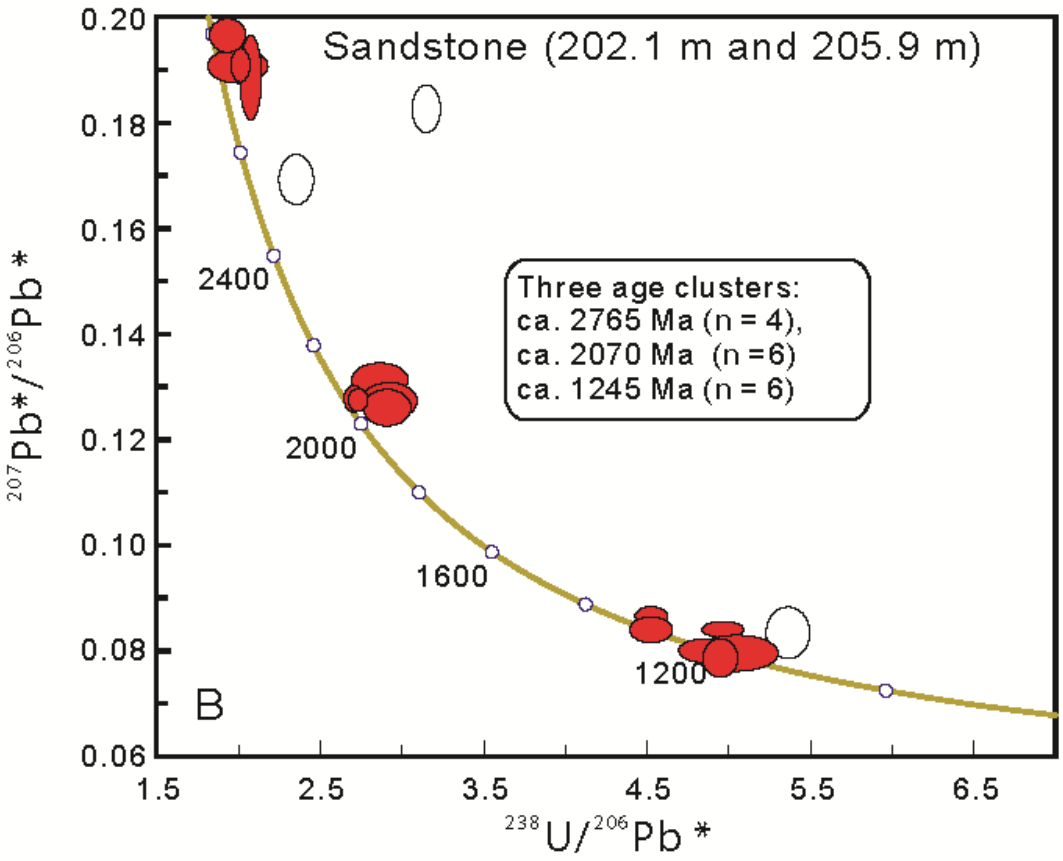

Figure DR9. Concordia plot for U-Pb analyses of zircon from the sandstone. Unfilled ellipses represent discordant analyses. Analyses giving high common Pb are not displayed but listed in Table DR3.

Fine-grained sandstone (Drill-hole W270, 283.3 m)

This sample of fine-grained sandstone was collected at drill-depth 283.3 m, ~53 m below the tuff bed. It contains zircons that are equant or elongate, subhedral crystals (Fig. DR10), with lengths of up to ~60 μm and aspect ratios of up to 2.5:1. Twelve analyses were performed on 7 zircon crystals (Table DR4). However, 4 of them record high common Pb fractions with f_{206} >1%, and another 4 analyses are >10% discordant. The remaining 4 analyses include 3 spots on 2 zircon grains yielding $^{238}U/^{206}Pb^*$ dates between 1224 ± 15 Ma (1σ) and 1160 ± 25 Ma (1σ), and an old outlier with a $^{207}Pb^*/^{206}Pb^*$ date of 2056 ± 20 Ma (1σ) (Fig. DR11).

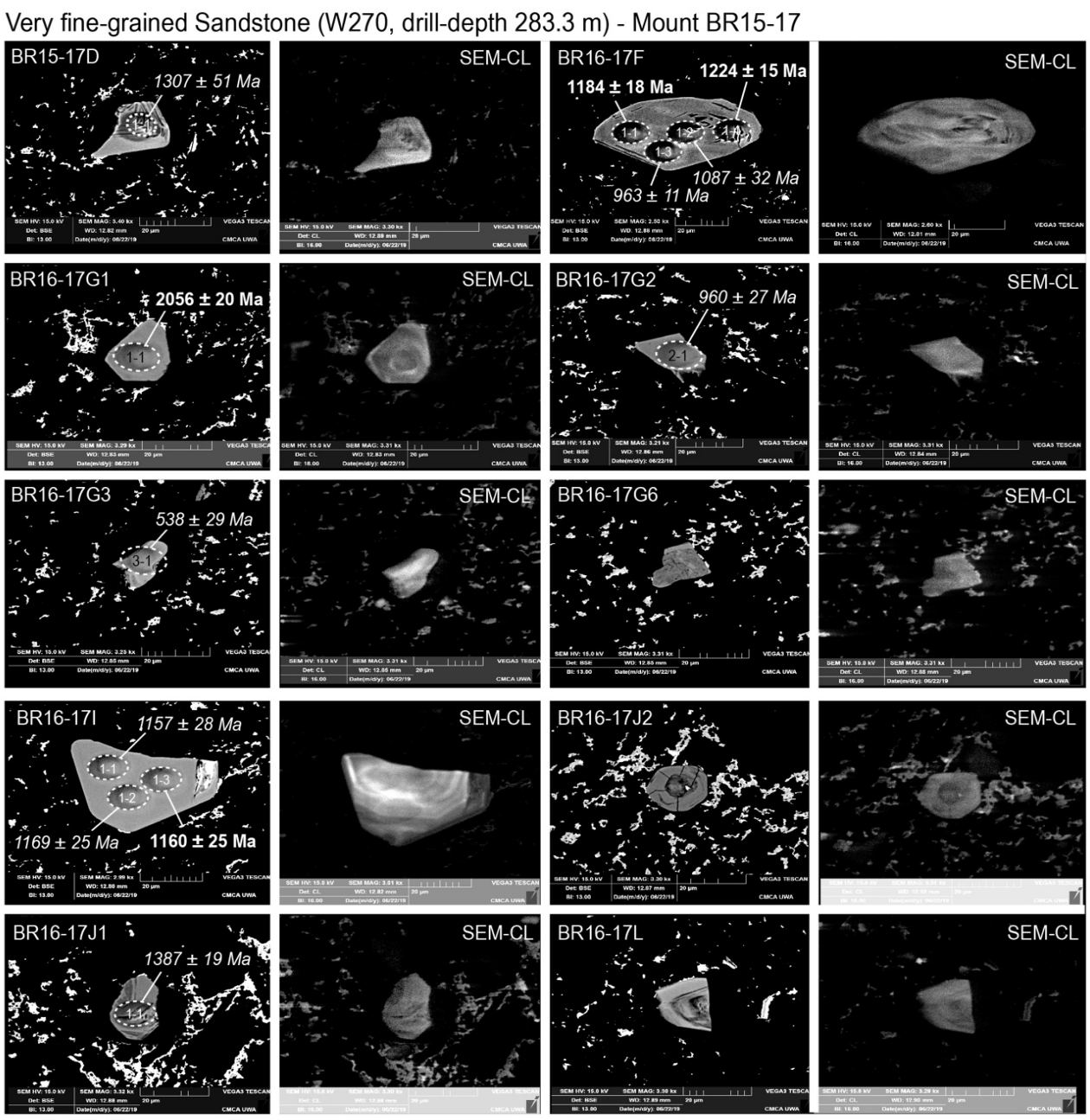

Figure DR10. SEM-backscattered electron (BSE) and cathodoluminescence (CL) images of detrital zircon grains drilled from fine-grained sandstones at drill-depth 283.3 m in drill-hole W270 (SHRIMP mount BR15-17 – Table DR4). The oval outlines on zircon grains mark ion microprobe analytical pits and are linked to corresponding $^{207}Pb/^{206}Pb$ or $^{238}U/^{206}Pb^*$ dates with 1σ analytical errors. Numbers in bold represent analyses that were used in age determinations, whereas numbers in italics were not used because of high common Pb contents and/or high levels of discordance.

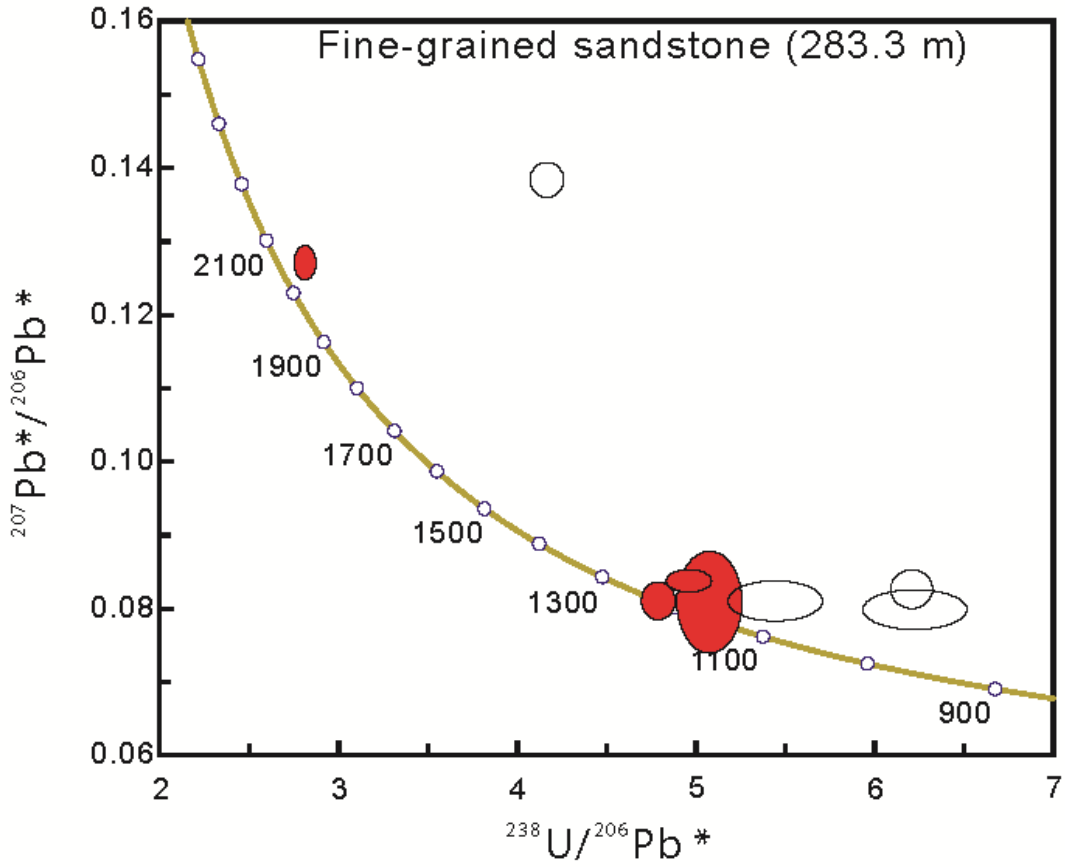

Figure DR11. Concordia plot for U-Pb analyses of detrital zircon from the fine-grained sandstone. Unfilled ellipses represent discordant analyses. Analyses giving high common Pb are not shown but listed in Table DR4.

Basal conglomerate (Drill-hole W270, 296.1 m)

Detrital zircons from the conglomerate near the base of the Mapedi Formation in W270 are typically large, rounded grains or crystal fragments with lengths of up to 200 μm (Fig. DR12). They have highly variable U and Th concentrations (33-1920 ppm and 33-1202 ppm, respectively) with Th/U ratios varying from 0.19-1.70. Eleven of the 38 analyses obtained on these zircons are disregarded as 4 of them contain high common Pb (f_{206} >1%) and the other 7 are >10% discordant (Table DR6). The remaining analyses yielded $^{207}Pb^*/^{206}Pb^*$ dates ranging from 3210 Ma to 1871 Ma with a prominent cluster at 2.0 Ga (Fig. DR13).

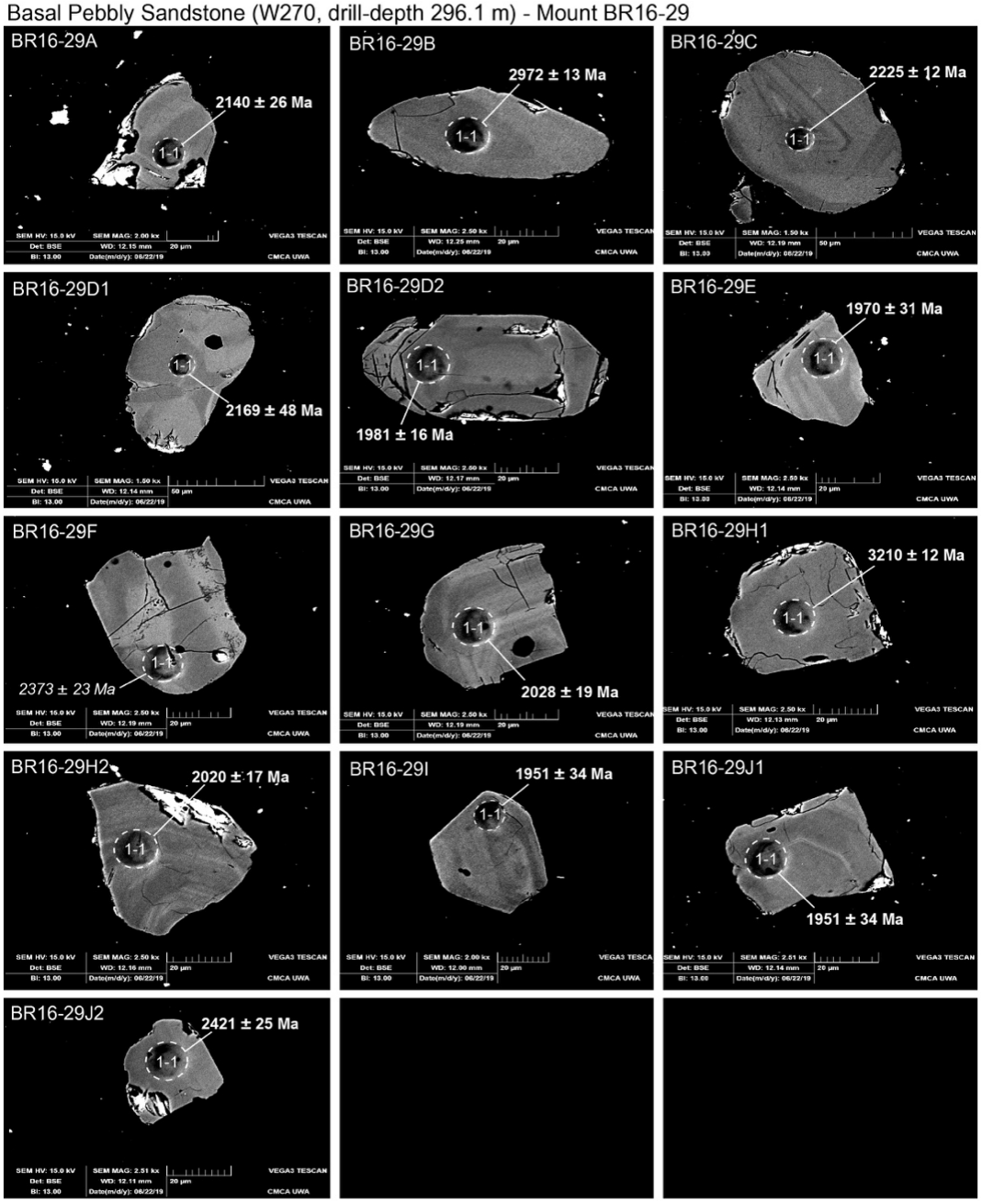

Figure DR12. SEM-backscattered electron (BSE) and cathodoluminescence (CL) images of detrital zircon grains drilled from a coarse-grained pebbly sandstone at drill-depth 296.1 m in drill-hole W270 (SHRIMP mount BR16-29 – Table DR6). The oval outlines on zircon grains mark ion microprobe analytical pits and are linked to corresponding $^{207}Pb/^{206}Pb$ or $^{238}U/^{206}Pb^*$ dates with 1σ analytical errors. Numbers in bold represent analyses that were used in age determinations, whereas numbers in italics were not used because of high common Pb contents and/or high levels of discordance.

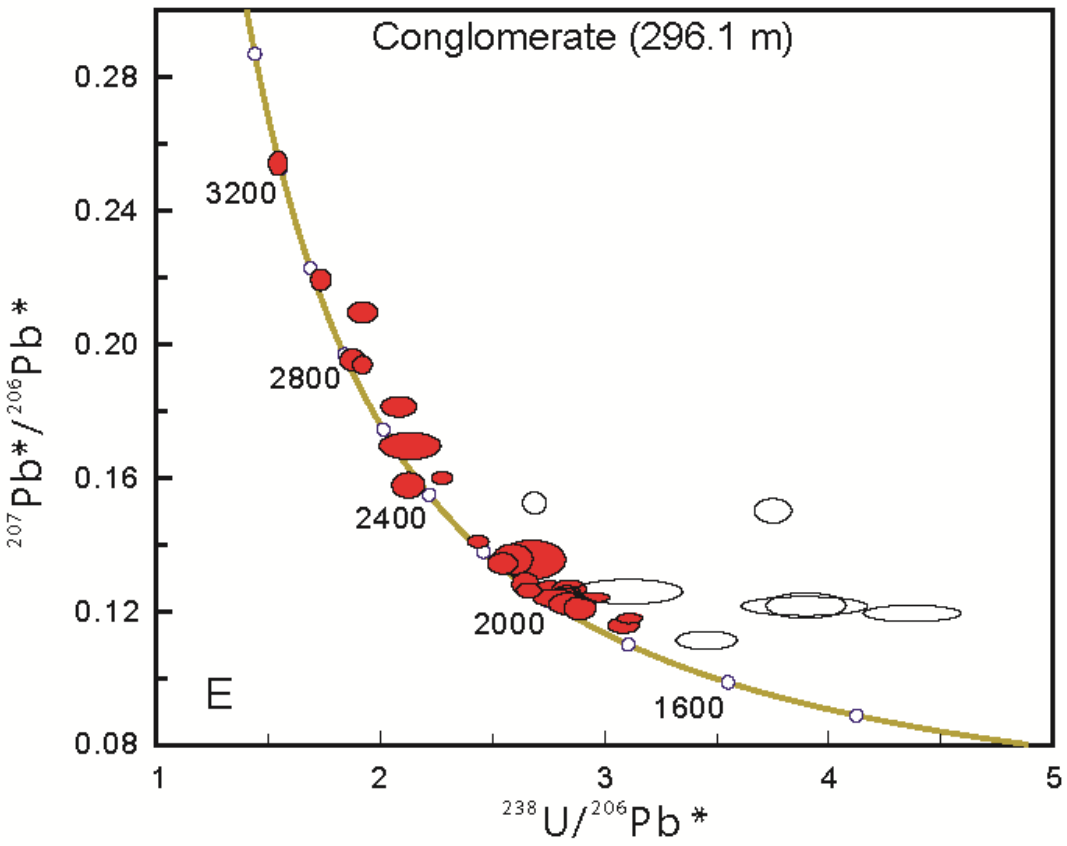

Figure DR13. Concordia plot for U-Pb analyses of detrital zircon from a coarse-grained, pebbly sandstone. Unfilled ellipses represent discordant analyses. Analyses giving high common Pb are not displayed but can be found in Table DR6.

Table DR1. SHRIMP operating parameters for all analytical sessions

Session	Date	Mount	Rock unit (depth in drill core W270)	Kohler aperture (µm)	Spot size (µm)	O_2^- primary (nA)	M/ΔM (1%)	No. of scans	No. of Pb/U standards (BR266)	Pb/U external precision (1σ, %)	IMF monitor (OG1)	IMF correctio
1	12/08/2015	BR15-19	sandstone (205.9 m)	50	12	-0.4	5500	8	9/9	1.00	3452 ± 14 Ma (n = 5)	Yes
2	09/09/2015	BR15-17 BR15-20 BR15-21	sandstone (283.3 m) sandstone (202.1 m) tuff (229.9 m)	50	12	-0.8	5170	7	21/22	1.00	3462 ± 5 Ma (n = 10)	No
3	08/02/2016	BR16-05	tuff (229.9 m)	50	12	-0.4	5500	7	6/7	2.11	3459 ± 15 Ma (n = 3)	No
4	03/08/2016	BR16-21 BR16-22 BR16-27 BR16-28	quartzite (184.1 m) quartzite (184.1 m) tuff (229.9 m) tuff (229.9 m)	30	10	-0.2	5200	8	22/22	1.65	3463 ± 10 Ma (n = 12)	No
5	13/10/2016	BR16-24 BR16-29 BR16-30 BR16-31	tuff (229.9 m) conglomerate conglomerate conglomerate	70	15	-1.0	4940	7	12/12	1.04	3476 ± 8 Ma (n = 5)	Yes

Table DR2. SHRIMP U-Pb data for zircon from a tuff bed in the Mapedi Formation (W270, 229.9 m)

					Total ratios				^{204}Pb corrected ratios				Ages (Ma)				
Analysis No.	**U (ppm)**	**Th (ppm)**	**Th/U**	**f_{206} (%)**	**^{238}U /^{206}Pb**	**±**	**^{207}Pb /^{206}Pb**	**±**	**^{238}U /^{206}Pb***	**±**	**^{207}Pb* /^{206}Pb***	**±**	**^{238}U /^{206}Pb***	**±**	**^{207}Pb* /^{206}Pb***	**±**	**Disc. (%)**
f_{206} <1%, disc. within ± 10%																	
Old outliers																	
1627E.1-3	184	129	0.70	0.50	3.179	0.089	0.1166	0.0024	3.195	0.089	0.1122	0.0035	1755	43	**1836**	**57**	5
1628F.1-3	117	149	1.27	0.00	3.172	0.088	0.1082	0.0023	3.172	0.088	0.1082	0.0023	1767	43	**1769**	**39**	0
1624F.1-1	181	149	0.82	0.00	3.287	0.049	0.1085	0.0011	3.287	0.049	0.1078	0.0011	1712	22	**1762**	**19**	3
1627G.1-2	82	50	0.61	0.40	3.553	0.137	0.1089	0.0036	3.567	0.138	0.1055	0.0050	1593	55	**1723**	**88**	8
1624F.1-2	180	106	0.59	0.22	4.012	0.059	0.0998	0.0011	4.021	0.059	0.0972	0.0014	1432	19	**1571**	**27**	9
Main population																	
1628I.1-1	296	222	0.75	0.31	4.443	0.096	0.0868	0.0015	4.456	0.097	0.0842	0.0021	**1305**	**26**	1296	50	-1
1628D.1-1	216	137	0.63	0.73	4.464	0.137	0.0865	0.0018	4.497	0.138	0.0803	0.0033	**1294**	**36**	1204	81	-8
1627C.1-2	340	223	0.66	0.37	4.495	0.108	0.0833	0.0020	4.511	0.109	0.0802	0.0030	**1291**	**28**	1202	73	-8
1628H.1-1	319	75	0.24	0.39	4.517	0.096	0.0824	0.0014	4.534	0.097	0.0791	0.0022	**1285**	**25**	1175	54	-10
1605G.1-2	54	25	0.47	0.37	4.538	0.163	0.0849	0.0043	4.538	0.163	0.0849	0.0043	**1284**	**42**	1312	99	2
1628E.1-1	226	164	0.73	0.59	4.557	0.105	0.0848	0.0018	4.584	0.107	0.0798	0.0031	**1272**	**27**	1192	76	-7
1624E.1-2	108	72	0.69	-0.08	4.634	0.081	0.0839	0.0015	4.630	0.081	0.0846	0.0017	**1261**	**20**	1307	38	4
1605G.1-3	78	36	0.46	0.27	4.649	0.150	0.0867	0.0034	4.649	0.150	0.0867	0.0034	**1256**	**37**	1353	77	8
1627C.1-1	196	93	0.47	0.32	4.636	0.133	0.0835	0.0054	4.650	0.134	0.0808	0.0060	**1256**	**33**	1216	147	-4
1628I.1-2	178	84	0.47	0.37	4.636	0.114	0.0817	0.0020	4.653	0.115	0.0786	0.0030	**1255**	**28**	1161	75	-9
1627F.1-3	156	46	0.30	1.00	4.607	0.119	0.0885	0.0037	4.653	0.122	0.0801	0.0053	**1255**	**30**	1200	131	-5
1624E.1-3	106	54	0.52	0.52	4.645	0.085	0.0878	0.0017	4.669	0.086	0.0834	0.0026	**1251**	**21**	1278	62	2
1605G.1-1	74	38	0.52	0.81	4.702	0.156	0.0784	0.0047	4.702	0.156	0.0784	0.0047	**1243**	**37**	1156	119	-8
1628A.1-1	340	345	1.02	0.25	4.724	0.107	0.0889	0.0032	4.736	0.107	0.0867	0.0036	**1235**	**26**	1355	79	10
1624E.1-1	100	57	0.60	-0.43	4.792	0.084	0.0830	0.0015	4.772	0.085	0.0867	0.0022	**1227**	**20**	1354	50	10
1627H.1-4	316	112	0.35	0.22	4.778	0.104	0.0820	0.0015	4.789	0.105	0.0801	0.0020	**1223**	**24**	1199	50	-2
1627F.1-6	295	133	0.45	0.66	4.772	0.108	0.0836	0.0017	4.804	0.110	0.0781	0.0030	**1219**	**25**	1148	77	-7
1627F.1-5	174	91	0.53	0.24	4.810	0.129	0.0881	0.0024	4.822	0.129	0.0861	0.0031	**1215**	**30**	1340	70	10
1627D.1-1	127	55	0.43	0.64	4.884	0.179	0.0886	0.0039	4.916	0.183	0.0832	0.0067	**1194**	**40**	1274	157	7
1627H.1-3	315	120	0.38	0.30	4.925	0.135	0.0850	0.0015	4.940	0.136	0.0824	0.0021	**1188**	**30**	1255	50	6

1628H.1-2	499	331	0.66	0.41	4.930	0.097	0.0853	0.0011	4.950	0.097	0.0818	0.0017	**1186**	**21**	1241	42	5
1605G.1-4	118	139	1.17	0.00	5.164	0.151	0.0810	0.0021	5.164	0.151	0.0810	0.0021	**1141**	**31**	1223	51	7
f_{206} <1%, disc. >10%																	
1627E.1-2	146	90	0.62	0.00	5.645	0.178	0.1113	0.0039	5.645	0.178	0.1113	0.0039	1051	31	1820	64	46
1627F.1-4	173	91	0.53	0.21	4.676	0.120	0.0787	0.0021	4.686	0.121	0.0769	0.0028	1247	29	1118	71	-13
1521B.1-1	159	97	0.61	0.22	4.954	0.080	0.0867	0.0015	4.965	0.081	0.0848	0.0020	1183	18	1311	46	11
1521B.1-2	433	350	0.81	0.32	6.218	0.162	0.0915	0.0011	6.238	0.162	0.0887	0.0016	959	23	1399	34	34
1628D.1-2	170	144	0.85	0.34	4.449	0.109	0.0811	0.0019	4.464	0.110	0.0782	0.0028	1303	29	1151	72	-15
1628B.1-1	182	111	0.61	0.45	4.565	0.120	0.0820	0.0032	4.585	0.121	0.0782	0.0042	1272	30	1152	106	-11
1628C.1-1	149	99	0.66	0.59	4.584	0.160	0.0826	0.0020	4.612	0.162	0.0776	0.0036	1265	40	1137	91	-12
1624F.1-3	195	94	0.48	0.72	4.083	0.059	0.1084	0.0012	4.113	0.060	0.1014	0.0020	1403	18	1650	36	15
1627H.1-1	345	119	0.35	0.87	4.620	0.117	0.0823	0.0022	4.661	0.119	0.0750	0.0043	1253	29	1068	115	-19
f_{206} >1%																	
1628F.1-1	107	101	0.94	1.09	3.246	0.096	0.1054	0.0026	3.281	0.098	0.0961	0.0050	1715	45	1549	97	-12
1628F.1-2	86	84	0.98	1.12	3.347	0.101	0.1128	0.0027	3.385	0.104	0.1031	0.0052	1669	45	1681	93	1
1628C.1-2	25	11	0.43	1.17	4.464	0.311	0.0931	0.0090	4.516	0.319	0.0832	0.0135	1289	83	1274	317	-1
1627F.1-2	167	89	0.54	1.19	4.652	0.146	0.0836	0.0030	4.708	0.151	0.0736	0.0066	1242	36	1032	181	-22
1627H.1-2	295	96	0.33	1.30	4.623	0.118	0.0785	0.0020	4.684	0.122	0.0678	0.0049	1247	30	861	151	-49
1521H.1-2	403	259	0.64	1.36	6.330	0.122	0.1172	0.0025	6.417	0.124	0.1054	0.0032	934	17	1721	56	49
1627E.1-1	170	73	0.43	1.53	3.104	0.091	0.1186	0.0028	3.152	0.095	0.1053	0.0058	1776	47	1720	102	-4
1627F.1-1	287	115	0.40	1.79	4.508	0.163	0.0832	0.0022	4.590	0.168	0.0684	0.0058	1271	42	880	175	-49
1521F.1-2	597	296	0.50	1.82	4.841	0.086	0.1060	0.0019	4.930	0.088	0.0905	0.0029	1190	19	1435	60	19
1627G.1-1	82	44	0.54	2.03	3.353	0.132	0.1177	0.0042	3.423	0.140	0.1001	0.0100	1652	59	1626	185	-2
1628A.1-2	146	99	0.68	2.10	4.637	0.212	0.0892	0.0029	4.737	0.220	0.0716	0.0079	1235	52	975	225	-29
1627D.1-2	87	37	0.42	2.46	4.760	0.191	0.0899	0.0044	4.880	0.209	0.0695	0.0129	1202	47	913	383	-35
1627A.1-1	112	47	0.42	2.48	3.139	0.107	0.1010	0.0029	3.218	0.114	0.0800	0.0082	1744	54	1198	201	-52
1521H.1-1	463	271	0.58	2.69	5.266	0.198	0.1240	0.0011	5.412	0.204	0.1007	0.0029	1093	38	1638	53	36
1521F.1-1	437	631	1.44	2.91	6.653	0.173	0.1086	0.0011	6.852	0.180	0.0839	0.0034	878	22	1291	80	34
1628B.2-1	103	148	1.43	3.34	3.405	0.103	0.1158	0.0030	3.522	0.112	0.0873	0.0088	1611	45	1367	193	-20

Pb* indicate radiogenic Pb

f_{206} is the proportion of common (unradiogenic) Pb in ^{206}Pb, determined using the measured ^{204}Pb/^{206}Pb and a common Pb composition from the Stacey and Kramers (1975) model at the approximate age of the sample.

$^{238}U/^{206}Pb^*$ and $^{207}Pb^*/^{206}Pb^*$ ratios and dates have been corrected for common Pb.

Disc. is apparent discordance, as 100 ($t[^{207}Pb^*/^{206}Pb^*] - t[^{238}U/^{206}Pb^*]$) / $t[^{207}Pb^*/^{206}Pb^*]$.

Analyses are sorted by descending $t[^{207}Pb^*/^{206}Pb^*]$ for analyses older than 1400 Ma, and $t[^{238}U/^{206}Pb^*]$ for those younger than 1400 Ma, except those excluded in age calculation due to large discordance (and/or high common Pb).

Table DR3. SHRIMP U-Pb data for detrital zircon from the Mapedi Formation (W270, 202.1 m and 205.9 m)

Analysis No.	U (ppm)	Th (ppm)	Th/U	f_{206} (%)	Total ratios				^{204}Pb corrected ratios				Ages (Ma)				Disc. (%)
					^{238}U /^{206}Pb	±	^{207}Pb /^{206}Pb	±	^{238}U /^{206}Pb*	±	^{207}Pb* /^{206}Pb*	±	^{238}U /^{206}Pb*	±	^{207}Pb* /^{206}Pb*	±	
f_{206} <1%, disc. within ± 10%																	
1520F.1-1	69	35	0.50	0.00	1.910	0.072	0.1967	0.0022	1.910	0.072	0.1967	0.0022	2714	83	**2799**	**18**	4
1520F.1-2	80	49	0.61	0.06	1.989	0.039	0.1916	0.0020	1.990	0.039	0.1910	0.0021	2625	42	**2751**	**18**	6
1519I.2-1	182	103	0.57	0.22	1.969	0.121	0.1912	0.0018	1.974	0.121	0.1909	0.0020	2642	132	**2750**	**17**	4
1519A.1-1	212	249	1.17	0.00	2.051	0.044	0.1871	0.0051	2.051	0.044	0.1887	0.0051	2561	45	**2731**	**44**	6
1520L.1-1	113	67	0.59	0.00	2.585	0.044	0.1334	0.0025	2.585	0.044	0.1334	0.0025	2108	31	**2144**	**33**	2
1519C.1-1	217	125	0.57	0.19	2.840	0.114	0.1315	0.0016	2.845	0.114	0.1310	0.0019	1942	67	**2111**	**25**	8
1520B.1-1	190	220	1.16	0.44	2.677	0.041	0.1311	0.0012	2.689	0.041	0.1273	0.0017	2038	27	**2061**	**23**	1
1520L.1-2	220	109	0.50	0.16	2.710	0.039	0.1285	0.0012	2.714	0.039	0.1271	0.0014	2022	25	**2058**	**19**	2
1519I.1-1	217	71	0.33	0.43	2.892	0.112	0.1295	0.0016	2.904	0.112	0.1269	0.0021	1908	63	**2055**	**30**	7
1519D.1-1	240	128	0.53	0.23	2.885	0.098	0.1265	0.0017	2.892	0.098	0.1256	0.0021	1914	56	**2037**	**30**	6
1520G.2-2	210	204	0.97	0.00	4.517	0.066	0.0857	0.0012	4.517	0.066	0.0857	0.0012	**1289**	**17**	1332	28	4
1520G.2-1	197	198	1.00	0.22	4.507	0.088	0.0851	0.0012	4.517	0.088	0.0832	0.0017	**1289**	**23**	1273	39	-1
1520C.1-1	252	128	0.51	0.24	4.824	0.096	0.0812	0.0011	4.835	0.096	0.0792	0.0015	**1212**	**22**	1177	37	-3
1520E.1-1	209	144	0.69	0.88	4.898	0.069	0.0852	0.0012	4.942	0.071	0.0778	0.0024	**1188**	**15**	1141	61	-5
1519H.1-1	545	531	0.97	0.00	5.000	0.128	0.0828	0.0012	5.000	0.128	0.0836	0.0012	**1175**	**27**	1283	27	8
1519M.1-2	435	478	1.10	0.30	5.029	0.167	0.0805	0.0019	5.044	0.168	0.0787	0.0022	**1166**	**35**	1165	55	0
f_{206} <1%, disc. >10%																	
1519M.1-1	296	365	1.23	0.22	5.350	0.088	0.0845	0.0029	5.362	0.088	0.0834	0.0031	1102	17	1279	73	14
1519L.1-2	251	91	0.36	0.24	2.347	0.070	0.1776	0.0029	2.353	0.070	0.1770	0.0030	2283	57	2625	29	13
1519K.1-1	230	195	0.85	0.11	1.911	0.032	0.2570	0.0019	1.913	0.032	0.2582	0.0019	2711	37	3236	12	16
1519G.1-1	301	305	1.01	0.63	3.129	0.056	0.1954	0.0021	3.149	0.057	0.1914	0.0027	1778	28	2754	23	35
f_{206} >1%																	
1520K.1-1	297	195	0.66	1.59	5.327	0.071	0.0976	0.0056	5.413	0.074	0.0841	0.0062	1093	14	1294	144	17
1520C.1-2	305	171	0.56	1.21	5.077	0.089	0.0985	0.0018	5.139	0.091	0.0881	0.0028	1146	19	1385	62	19
1520F.2-1	283	323	1.14	6.88	5.781	0.077	0.1479	0.0015	6.208	0.094	0.0891	0.0066	963	14	1406	141	34
1520F.2-2	326	251	0.77	3.29	5.783	0.076	0.1208	0.0029	5.979	0.083	0.0925	0.0050	997	13	1478	103	35

1519E.1-2	219	276	1.26	1.41	6.540	0.247	0.0912	0.0036	6.633	0.253	0.0801	0.0056	905	32	1198	138	24
1519J.1-1	515	1049	2.04	1.42	3.161	0.044	0.1779	0.0030	3.207	0.045	0.1666	0.0035	1750	22	2524	36	31
1519L.1-1	783	454	0.58	5.21	6.384	0.159	0.1665	0.0034	6.734	0.175	0.1218	0.0077	893	22	1983	112	55
1519E.1-1	245	265	1.08	11.79	3.915	0.101	0.1571	0.0059	4.438	0.148	0.0611	0.0186	1310	39	642	653	-104
1519B.1-1	220	283	1.29	2.33	4.760	0.089	0.0830	0.0017	4.874	0.096	0.0643	0.0051	1203	22	753	166	-60
1519F.1-1	236	354	1.50	4.26	2.896	0.129	0.1345	0.0031	3.025	0.138	0.0986	0.0096	1841	73	1597	183	-15

Footnotes as in Table DR2.

Table DR4. SHRIMP U-Pb data for detrital zircon from fine-grained sandstone in the Mapedi Formation (W270, 283.3 m)

Analysis No.	U (ppm)	Th (ppm)	Th/U	f_{206} (%)	Total ratios				^{204}Pb corrected ratios				Ages (Ma)				Disc. (%)
					^{238}U /^{206}Pb	±	^{207}Pb /^{206}Pb	±	^{238}U /^{206}Pb*	±	^{207}Pb* /^{206}Pb*	±	^{238}U /^{206}Pb*	±	^{207}Pb* /^{206}Pb*	±	
f_{206} <1%, disc. within ± 10%																	
1517G.1-1	217	120	0.55	0.21	2.790	0.040	0.1280	0.0011	2.796	0.040	0.1270	0.0015	1971	24	**2056**	**20**	4
1517F.1-4	281	29	0.10	0.49	4.760	0.063	0.0842	0.0010	4.783	0.064	0.0805	0.0017	**1224**	**15**	1210	41	-1
1517F.1-1	332	73	0.22	0.00	4.958	0.084	0.0828	0.0009	4.958	0.084	0.0833	0.0010	**1184**	**18**	1276	23	7
1517I.1-3	46	38	0.82	0.80	5.030	0.118	0.0866	0.0024	5.070	0.122	0.0803	0.0046	**1160**	**25**	1205	113	4
f_{206} <1%, disc. >10%																	
1517F.1-2	294	257	0.87	0.56	5.412	0.173	0.0853	0.0010	5.443	0.174	0.0811	0.0018	1087	32	1223	44	11
1517G.2-1	432	211	0.49	0.85	6.172	0.190	0.0866	0.0009	6.225	0.192	0.0799	0.0018	960	27	1194	44	20
1517F.1-3	414	348	0.84	0.62	6.168	0.076	0.0874	0.0009	6.207	0.077	0.0826	0.0017	963	11	1261	40	24
1517J.1-1	386	241	0.62	0.43	4.148	0.062	0.1414	0.0010	4.166	0.062	0.1384	0.0015	1387	19	2207	19	37
f_{206} >1%																	
1517D.1-1	569	759	1.33	1.18	8.919	0.248	0.0941	0.0009	9.026	0.252	0.0846	0.0022	677	18	1307	51	48
1517G.3-1	703	464	0.66	1.31	11.33	0.632	0.0962	0.0012	11.479	0.642	0.0855	0.0026	538	29	1328	59	59
1517I.1-1	40	36	0.91	1.86	4.990	0.127	0.0789	0.0026	5.085	0.137	0.0639	0.0075	1157	28	740	247	-56
1517I.1-2	50	49	0.98	1.85	4.936	0.112	0.0854	0.0023	5.029	0.120	0.0704	0.0064	1169	25	940	186	-24

Footnotes as in Table DR2.

Table DR5. SHRIMP U-Pb data for detrital zircon in quartz arenite from the Mapedi Formation (W270, 184.1 m)

Analysis No.	U (ppm)	Th (ppm)	Th/U	f_{206} (%)	Total ratios				^{204}Pb corrected ratios				Ages (Ma)				Disc. (%)
					^{238}U /^{206}Pb	±	^{207}Pb /^{206}Pb	±	^{238}U /^{206}Pb*	±	^{207}Pb* /^{206}Pb*	±	^{238}U /^{206}Pb*	±	^{207}Pb* /^{206}Pb*	±	
f_{206} <1%, disc. within ± 5%																	
1621C.1-1	133	141	1.06	0.14	1.686	0.058	0.2440	0.0040	1.688	0.058	0.2428	0.0042	2999	83	3139	27	6
1621C.1-2	128	133	1.04	0.27	1.649	0.057	0.2322	0.0038	1.653	0.058	0.2298	0.0042	3050	85	**3051**	**29**	0
1622E.1-1	326	131	0.40	0.15	1.658	0.036	0.2282	0.0018	1.661	0.036	0.2268	0.0019	3039	53	**3030**	**13**	0
1622E.1-2	252	89	0.35	0.21	1.796	0.041	0.2201	0.0020	1.800	0.042	0.2183	0.0022	2849	53	**2968**	**16**	5
1622C.1-1	235	117	0.50	0.00	1.797	0.041	0.2139	0.0019	1.797	0.041	0.2139	0.0019	2852	53	**2936**	**15**	4
1621F.2-1	184	74	0.40	0.27	1.832	0.058	0.2018	0.0033	1.837	0.059	0.1994	0.0038	2801	73	**2822**	**31**	1
1621F.2-3	241	110	0.45	0.21	1.932	0.067	0.1973	0.0020	1.936	0.067	0.1955	0.0022	2684	76	**2789**	**19**	5
1621J.1-1	155	47	0.30	0.13	1.886	0.048	0.1944	0.0023	1.888	0.048	0.1932	0.0024	2740	56	**2770**	**20**	1
1621J.1-2	190	80	0.42	0.30	2.090	0.054	0.1894	0.0024	2.097	0.054	0.1868	0.0027	2514	53	2714	24	9
1622B.1-1	107	87	0.81	0.00	2.197	0.065	0.1702	0.0028	2.197	0.065	0.1702	0.0028	2418	59	2560	27	7
1621K.1-1	265	135	0.51	0.36	2.492	0.055	0.1460	0.0016	2.502	0.055	0.1428	0.0020	2168	41	**2261**	**24**	5
1621L.1-2	146	143	0.98	0.13	2.675	0.072	0.1362	0.0035	2.678	0.073	0.1351	0.0037	2045	47	2165	47	6
1621L.1-1	122	114	0.94	0.14	2.566	0.072	0.1356	0.0025	2.570	0.072	0.1344	0.0028	2119	51	**2156**	**36**	2
1621E.2-3	89	36	0.40	-0.20	2.696	0.093	0.1309	0.0029	2.691	0.093	0.1326	0.0034	2037	60	**2133**	**45**	5
1622G.1-1	209	118	0.57	0.23	2.573	0.065	0.1327	0.0022	2.579	0.065	0.1307	0.0026	2112	46	**2107**	**36**	0
1622G.1-2	170	99	0.58	0.31	2.522	0.088	0.1326	0.0021	2.529	0.089	0.1299	0.0026	2148	64	**2097**	**35**	-3
1622H.1-2	157	103	0.66	0.19	2.549	0.065	0.1316	0.0020	2.553	0.066	0.1299	0.0023	2130	47	**2097**	**31**	-2
1622I.1-3	101	65	0.64	0.33	2.724	0.082	0.1325	0.0026	2.733	0.082	0.1296	0.0033	2010	52	**2093**	**45**	5
1621F.1-1	107	53	0.49	0.38	2.614	0.107	0.1329	0.0041	2.624	0.108	0.1296	0.0054	2081	73	**2092**	**73**	1
1621D.1-3	305	98	0.32	-0.07	2.621	0.058	0.1288	0.0017	2.620	0.058	0.1294	0.0018	2084	39	**2090**	**24**	0
1622I.1-1	150	149	0.99	0.67	2.672	0.071	0.1348	0.0022	2.690	0.072	0.1289	0.0033	2037	47	**2083**	**45**	3
1621G.1-1	92	67	0.73	0.00	2.687	0.108	0.1283	0.0040	2.687	0.108	0.1283	0.0040	2039	70	**2075**	**55**	2
1622H.1-1	175	61	0.35	0.36	2.566	0.069	0.1313	0.0038	2.575	0.069	0.1281	0.0042	2115	49	**2072**	**58**	-2
1622F.1-1	213	135	0.63	0.17	2.704	0.065	0.1285	0.0019	2.709	0.065	0.1269	0.0022	2025	42	**2056**	**30**	2
1622A.1-1	68	27	0.40	0.77	2.612	0.095	0.1333	0.0033	2.633	0.097	0.1265	0.0052	2076	65	**2050**	**72**	-1
1621E.2-2	104	42	0.40	0.36	2.620	0.079	0.1291	0.0027	2.629	0.079	0.1259	0.0036	2078	54	**2042**	**50**	-2
1621D.1-1	245	78	0.32	0.47	2.571	0.072	0.1298	0.0026	2.583	0.073	0.1257	0.0035	2110	51	**2038**	**50**	-4
1621I.1-1	129	71	0.55	0.35	2.591	0.069	0.1268	0.0022	2.601	0.069	0.1237	0.0029	2097	48	**2010**	**41**	-5
1622F.1-2	185	104	0.56	0.44	2.629	0.068	0.1273	0.0021	2.641	0.068	0.1234	0.0029	2070	46	**2007**	**42**	-4

1621I.1-2	142	80	0.56	0.39	2.660	0.073	0.1268	0.0040	2.670	0.073	0.1233	0.0045	2051	48	**2005**	**65**	-3
1621F.3-1	181	109	0.60	0.75	2.651	0.088	0.1299	0.0033	2.671	0.090	0.1233	0.0050	2050	59	**2004**	**73**	-3
1621G.1-2	89	67	0.75	0.00	2.843	0.119	0.1227	0.0039	2.843	0.119	0.1227	0.0039	1943	70	**1996**	**56**	3
1621E.2-1	89	36	0.40	0.74	2.671	0.110	0.1290	0.0059	2.691	0.112	0.1225	0.0076	2037	73	**1993**	**110**	-3
1621G.1-3	119	100	0.85	0.89	2.729	0.081	0.1292	0.0027	2.754	0.083	0.1214	0.0044	1997	52	**1978**	**65**	-1
1621A.1-3	136	106	0.77	0.35	2.904	0.082	0.1174	0.0025	2.914	0.082	0.1143	0.0033	1902	46	**1870**	**53**	-2
1621A.1-1	157	124	0.79	0.92	3.230	0.108	0.1149	0.0033	3.260	0.110	0.1069	0.0057	1725	51	**1747**	**98**	1
1622D.1-1	235	279	1.19	0.26	4.421	0.101	0.0864	0.0017	4.433	0.102	0.0842	0.0023	**1311**	**27**	1298	54	-1
1621H.1-1	137	208	1.52	0.21	4.488	0.161	0.0856	0.0022	4.497	0.161	0.0838	0.0029	**1294**	**42**	1288	67	-1
1622D.1-2	331	244	0.74	0.37	4.491	0.096	0.0877	0.0015	4.508	0.096	0.0845	0.0022	**1292**	**25**	1305	50	1
f_{206} <1%, disc. >5%																	
1621H.1-3	140	194	1.39	-0.59	4.565	0.127	0.0872	0.0026	4.538	0.127	0.0922	0.0044	1284	33	1472	90	14
1621H.1-2	114	109	0.96	-0.34	5.623	0.155	0.0919	0.0029	5.604	0.156	0.0949	0.0041	1058	27	1525	82	33
1621M.1-1	386	99	0.26	0.00	3.260	0.067	0.1255	0.0015	3.260	0.067	0.1255	0.0015	1725	31	2036	21	17
1622E.2-1	184	125	0.68	0.09	2.951	0.072	0.1305	0.0020	2.953	0.072	0.1297	0.0021	1880	40	2094	29	12
1622J.2-1	228	152	0.67	0.14	4.816	0.111	0.0899	0.0018	4.823	0.112	0.0888	0.0022	1215	26	1399	47	14
1621E.1-1	260	292	1.12	0.42	2.836	0.077	0.1465	0.0027	2.848	0.078	0.1429	0.0034	1940	46	2262	41	16
1621B.1-2	409	140	0.34	0.47	5.882	0.180	0.1299	0.0043	5.910	0.181	0.1257	0.0049	1008	29	2039	69	55
1621K.1-2	424	1061	2.50	0.50	4.616	0.133	0.1416	0.0023	4.639	0.134	0.1372	0.0027	1258	33	2192	34	47
1621D.1-4	623	174	0.28	0.60	6.098	0.119	0.1365	0.0016	6.135	0.120	0.1312	0.0023	973	18	2114	31	58
1621B.1-1	253	92	0.36	0.62	3.552	0.094	0.1252	0.0038	3.574	0.095	0.1198	0.0047	1590	37	1953	70	21
1621E.1-2	553	420	0.76	0.62	4.023	0.112	0.1367	0.0020	4.048	0.113	0.1312	0.0029	1423	36	2114	39	36
1621F.2-2	893	215	0.24	0.64	8.426	0.281	0.1933	0.0026	8.480	0.283	0.1876	0.0034	719	23	2721	30	78
f_{206} >1%																	
1622D.1-3	133	114	0.86	1.22	4.630	0.124	0.0896	0.0024	4.688	0.128	0.0793	0.0053	1247	31	1179	131	-6
1622I.1-2	64	27	0.42	1.31	2.758	0.140	0.1263	0.0030	2.795	0.143	0.1149	0.0056	1972	87	1879	88	-6
1621A.1-2	119	90	0.76	1.35	3.720	0.129	0.1186	0.0063	3.771	0.134	0.1068	0.0087	1516	48	1746	150	15
1622J.1-11	1529	409	0.27	1.47	11.97	0.239	0.1290	0.0019	12.14	0.244	0.1161	0.0031	510	10	1898	48	76
1622A.1-2	76	36	0.48	1.78	2.569	0.087	0.1297	0.0032	2.615	0.090	0.1141	0.0068	2087	61	1866	108	-14
1621H.1-4	73	34	0.46	1.89	4.820	0.260	0.0867	0.0037	4.913	0.271	0.0710	0.0100	1194	60	957	289	-27
1621D.1-2	751	161	0.21	2.29	8.123	0.169	0.1359	0.0023	8.313	0.179	0.1159	0.0052	732	15	1894	81	65

Footnotes as in Table DR2.

Table DR6. SHRIMP U-Pb data for detrital zircon from basal pebbly sandstone, Mapedi Formation (W270, 296.1 m)

Analysis No.	U (ppm)	Th (ppm)	Th/U	f_{206} (%)	Total ratios $^{238}U/^{206}Pb$	±	Total ratios $^{207}Pb/^{206}Pb$	±	^{204}Pb corrected ratios $^{238}U/^{206}Pb^*$	±	^{204}Pb corrected ratios $^{207}Pb^*/^{206}Pb^*$	±	Ages (Ma) $^{238}U/^{206}Pb^*$	±	Ages (Ma) $^{207}Pb^*/^{206}Pb^*$	±	Disc. (%)
f_{206} <1%, disc. within ± 5%																	
1629H.1-1	85	64	0.75	-0.11	1.529	0.027	0.2548	0.0019	1.528	0.027	0.2540	0.0019	3246	44	**3210**	**12**	-1
1629B.1-1	76	47	0.62	0.06	1.719	0.030	0.2209	0.0018	1.720	0.030	0.2188	0.0018	2955	41	**2972**	**13**	1
1630H.1-1	248	105	0.43	0.08	3.455	0.090	0.1121	0.0017	1.921	0.044	0.2094	0.0017	2702	50	2901	13	7
1631C.1-1	73	38	0.52	0.00	1.862	0.037	0.1959	0.0020	1.862	0.037	0.1946	0.0020	2771	44	**2781**	**16**	0
1631D.1-1	149	46	0.31	0.02	1.905	0.030	0.1947	0.0014	1.906	0.030	0.1931	0.0014	2719	35	**2769**	**12**	2
1631E.1-1	94	37	0.39	0.08	2.069	0.053	0.1824	0.0017	2.070	0.053	0.1804	0.0018	2540	54	**2657**	**16**	4
1631F.1-1	182	80	0.44	0.05	2.120	0.091	0.1703	0.0025	2.121	0.091	0.1686	0.0025	2490	88	**2544**	**25**	2
1630J.2-1	272	130	0.48	0.00	2.264	0.030	0.1601	0.0009	2.264	0.030	0.1590	0.0009	2358	26	**2445**	**9**	4
1629J.2-1	44	75	1.70	0.15	2.109	0.049	0.1592	0.0021	2.112	0.049	0.1568	0.0023	2499	48	**2421**	**25**	-3
1629C.1-1	199	92	0.46	0.06	2.426	0.033	0.1413	0.0009	2.427	0.033	0.1398	0.0010	2224	25	**2225**	**12**	0
1629D.1-1	33	33	1.00	0.67	3.875	0.117	0.1279	0.0022	2.675	0.099	0.1354	0.0038	2048	65	2169	48	6
1631J.1-1	142	129	0.91	-0.08	2.582	0.060	0.1346	0.0029	2.580	0.060	0.1344	0.0030	2112	42	**2156**	**39**	2
1629A.1-1	193	70	0.36	0.02	2.532	0.045	0.1343	0.0020	2.533	0.045	0.1331	0.0020	2145	32	**2140**	**26**	0
1631H.2-1	169	149	0.88	0.14	2.637	0.040	0.1291	0.0021	2.640	0.040	0.1270	0.0022	2071	27	**2057**	**30**	-1
1630G.2-1	186	90	0.48	-0.09	2.749	0.040	0.1259	0.0011	2.747	0.040	0.1258	0.0012	2001	25	**2040**	**17**	2
1630B.1-1	80	81	1.01	-0.06	2.836	0.051	0.1257	0.0016	2.834	0.051	0.1254	0.0017	1948	30	**2035**	**24**	4
1629G.1-1	235	132	0.56	-0.02	2.653	0.035	0.1256	0.0014	2.652	0.035	0.1249	0.0014	2063	23	**2028**	**19**	-2
1629H.2-1	172	90	0.53	-0.03	2.824	0.041	0.1250	0.0012	2.824	0.041	0.1244	0.0012	1954	24	**2020**	**17**	3
1630G.1-1	108	97	0.90	0.06	2.809	0.047	0.1246	0.0015	2.811	0.047	0.1232	0.0015	1962	28	**2003**	**22**	2
1630D.1-1	442	424	0.96	0.14	2.926	0.056	0.1250	0.0007	2.930	0.056	0.1229	0.0008	1893	31	**1999**	**11**	5
1631G.1-1	475	146	0.31	0.06	2.769	0.063	0.1241	0.0016	2.771	0.063	0.1227	0.0016	1987	39	**1996**	**23**	0
1631J.3-1	417	215	0.52	0.03	2.844	0.035	0.1235	0.0007	2.845	0.035	0.1224	0.0008	1942	21	**1992**	**11**	3
1629D.2-1	149	119	0.80	0.03	2.846	0.041	0.1228	0.0011	2.847	0.041	0.1216	0.0011	1940	24	**1981**	**16**	2
1629E.1-1	121	98	0.81	0.00	2.837	0.062	0.1218	0.0021	2.837	0.062	0.1209	0.0021	1946	36	**1970**	**31**	1
1629I.1-1	100	102	1.02	-0.05	2.884	0.047	0.1200	0.0022	2.883	0.047	0.1196	0.0023	1920	27	**1951**	**34**	2
1630J.1-1	383	211	0.55	0.07	1.919	0.044	0.2116	0.0017	3.111	0.038	0.1179	0.0008	1797	19	1924	12	7
1629J.1-1	124	121	0.97	0.13	3.072	0.047	0.1163	0.0012	3.076	0.047	0.1144	0.0014	1815	24	**1871**	**22**	3

f_{206} <1%, disc. >5%																	
1631A.1-1	91	58	0.64	0.00	2.657	0.098	0.1423	0.0026	3.455	0.090	0.1113	0.0017	1639	38	1821	28	10
1631B.1-1	362	68	0.19	0.04	3.109	0.038	0.1193	0.0007	3.891	0.186	0.1215	0.0016	1475	63	1979	24	25
1629F.1-1	276	140	0.51	0.09	3.095	0.160	0.1294	0.0018	2.687	0.035	0.1524	0.0020	2040	23	2373	23	14
1631G.2-1	92	59	0.65	0.30	2.684	0.035	0.1543	0.0020	3.104	0.161	0.1258	0.0022	1800	81	2041	31	12
1630C.1-1	298	232	0.78	0.61	3.889	0.186	0.1228	0.0016	3.898	0.118	0.1217	0.0024	1472	40	1981	35	26
1630A.1-1	360	164	0.46	0.73	4.340	0.143	0.1266	0.0009	4.371	0.144	0.1194	0.0014	1328	39	1947	21	32
1631J.2-1	579	244	0.42	0.82	3.719	0.054	0.1584	0.0020	3.750	0.055	0.1501	0.0023	1524	20	2347	26	35
f_{206} >1%																	
1630C.2-1	769	1202	1.56	1.09	9.535	0.203	0.1198	0.0011	8.868	0.454	0.1240	0.0016	689	33	2014	23	66
1630E.1-1	166	168	1.01	1.22	7.785	0.172	0.1455	0.0022	3.373	0.051	0.1112	0.0029	1674	22	1820	47	8
1630K.1-1	597	394	0.66	1.55	8.771	0.449	0.1344	0.0009	7.908	0.175	0.1309	0.0029	768	16	2109	39	64
1631G.3-1	1920	867	0.45	1.77	3.332	0.050	0.1226	0.0021	9.707	0.207	0.1037	0.0017	632	13	1691	30	63

Footnotes as in Table DR2.

REFERENCES CITED

Fletcher, I.R., McNaughton, N.J., Davis, W.J., and Rasmussen, B., 2010, Matrix effects and calibration limitations in ion probe U-Pb and Th–Pb dating of monazite: Chemical Geology, v. 270, p. 31–44.

Ludwig, K.R., 2008, Isoplot 3.6; a geochronology toolkit for Microsoft Excel. Berkeley Geochronology Center, 77 pp.

Ludwig, K.R., 2009, Squid 2; A User's Manual. Berkeley Geochronology Center, 100 pp.

Stacey, J.S., and Kramers, J.D., 1975, Approximation of terrestrial lead isotope evolution by a two-stage model: Earth and Planetary Science Letters, v. 26, p. 207–221.

Stern, R.A., 2001, A new isotopic and trace-element standard for the ion microprobe: Preliminary thermal ionization mass spectrometry (TIMS) U\Pb and electron microprobe data. Radiogenic Age and Isotopic Studies, Report 14: Geological Survey of Canada, Current Research 2001–F1, 11 pp.

Stern, R.A., Bodorkos, S., Kamo, S.L., Hickman, A.H., and Corfu, F., 2009, Measurement of SIMS instrumental mass fractionation of Pb isotopes during zircon dating: Geostandards and Geoanalytical Research, v. 33, p. 145–168.